

MetaOcc: Surround-View 4D Radar and Camera Fusion Framework for 3D Occupancy Prediction with Dual Training Strategies

Long Yang*, Lianqing Zheng*, Wenjin Ai, Minghao Liu, Sen Li, Qunshu Lin, Shengyu Yan, Jie Bai, Zhixiong Ma[†], Xichan Zhu

Abstract—3D occupancy prediction is crucial for autonomous driving perception. Fusion of 4D radar and camera provides a potential solution of robust occupancy prediction on serve weather with least cost. How to achieve effective multi-modal feature fusion and reduce annotation costs remains significant challenges. In this work, we propose MetaOcc, a novel multi-modal occupancy prediction framework that fuses surround-view cameras and 4D radar for comprehensive environmental perception. We first design a height self-attention module for effective 3D feature extraction from sparse radar points. Then, a local-global fusion mechanism is proposed to adaptively capture modality contributions while handling spatio-temporal misalignments. Temporal alignment and fusion module is employed to further aggregate historical feature. Furthermore, we develop a semi-supervised training procedure leveraging open-set segmentor and geometric constraints for pseudo-label generation, enabling robust perception with limited annotations. Extensive experiments on OmniHD-Scenes dataset demonstrate that MetaOcc achieves state-of-the-art performance, surpassing previous methods by significant margins. Notably, as the first semi-supervised 4D radar and camera fusion-based occupancy prediction approach, MetaOcc maintains 92.5% of the fully-supervised performance while using only 50% of ground truth annotations, establishing a new benchmark for multi-modal 3D occupancy prediction. Code and data are available at <https://github.com/LucasYang567/MetaOcc>.

Index Terms—Autonomous driving, multi-modal fusion, 4D radar, semi-supervised learning, occupancy prediction.

I. INTRODUCTION

The core challenge in autonomous driving is to achieve comprehensive scene understanding through robust 3D perception. Despite significant progress, 3D object detection struggles with unconventional obstacles [1]. 3D occupancy prediction advances next-generation perception by providing geometric-semantic representations for complex scenes [2].

Furthermore, perception performance is limited by sensor characteristics. While cameras provide dense semantic infor-

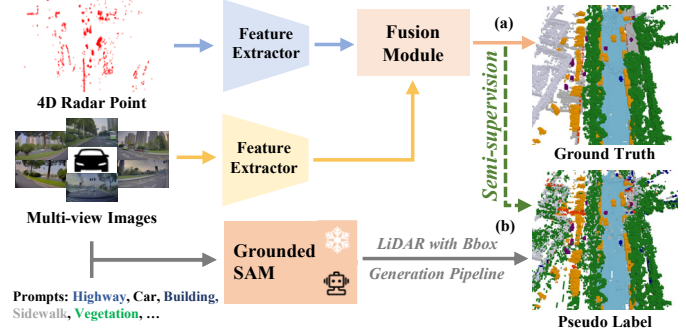


Fig. 1: The overview of MetaOcc. (a) The occupancy prediction framework that leverages surround-view 4D radar and camera fusion for robust 3D scene understanding. (b) Semi-supervised learning strategy utilizing Grounded-SAM to generate pseudo-labels, significantly reducing annotation costs while maintaining competitive performance.

mation but degrade in adverse conditions, LiDAR offers precise geometric measurements at high cost. The emerging high-resolution 4D imaging radar inherits the robustness and cost-effectiveness of traditional radar while incorporating elevation measurements [3], [4]. Compared with LiDAR, 4D radar demonstrates superior capabilities in capturing dynamic objects, enhancing driving safety [5], [6]. The fusion of surround-view cameras and 4D radar shows promising potential for robust occupancy prediction in adverse conditions.

Recent advancement of camera and 4D radar fusion has produced considerable success on perception [6]–[9], yet camera and 4D radar fusion for occupancy prediction remains largely unexplored, as existing 4D radar datasets [10], [11] lack both surround-view coverage and occupancy annotations. OmniHD-Scenes [4] dataset addresses limitation by providing multi-view radar data and comprehensive occupancy labels. Most camera-LiDAR approaches [12]–[14] adopt voxel-based methods to extract spatial feature for point cloud and conduct multi-modal fusion in unified space. However, compared to LiDAR, 4D radar point clouds exhibit increased sparsity and divergence, where voxelization introduces more void regions and limits effective feature extraction. Furthermore, significant challenges persist in achieving robust multi-modal fusion, particularly in modal contribution weighting and spatio-temporal misalignment caused by sensor calibration and temporal asynchronization.

The generation of 3D occupancy ground truth heavily relies on point-wise LiDAR segmentation [4], [13], [15], leading to substantial annotation costs. Several self-supervised ap-

* Both authors contribute equally to the work and are co-first authors.

[†] Corresponding Author.

Long Yang, Lianqing Zheng, Wenjin Ai, Zhixiong Ma, Xichan Zhu, are with the School of Automotive Studies, Tongji University, Shanghai 201804, China. E-mail: {yanglong, zhenglianqing, 2332971, zhuxichan, mzx1978}@tongji.edu.cn.

Minghao Liu is with the 2077AI Foundation, Singapore. E-mail: dreamforever.liu@gmail.com.

Sen Li is with Autonomous Driving Development, NIO, China. E-mail: sen.lee@nio.com

Qunshu Lin is with the College of Computer Science and Technology, Zhejiang University, Hangzhou 310027, China. E-mail: jacklin@abaka.ai

Shengyu Yan is with the school of automobile, Chang’an University, Xi’an, Shaanxi, 710018, China. Email: ysy@chd.edu.cn

Jie Bai is with the School of Information and Electrical Engineering, Hangzhou City University, Hangzhou 310015, China. E-mail: baij@zucc.edu.cn.

proaches [16], [17] leverage neural rendering and geometric consistency, but face notable limitations in dynamic object and complex environments for occupancy prediction. Recent advances [18] in open-set segmentor suggest promising direction for cost-effective occupancy label generation through text prompts, despite limitations in handling small objects and occluded scenarios.

To address above challenges, we propose MetaOcc, a surround-view occupancy prediction framework that fuses 4D radar and camera, as shown in Fig. 1. Our framework comprises Radar Height Self-attention (RHS) module effectively extracting 3D features from inherently sparse 4D radar points. MetaOcc Fusion Module (MFM) combines Local Adaptive Fusion (LAF) to capture modal contributions and Global Cross-attention Fusion (GCF) to handle spatio-temporal misalignment through deformable attention. Additionally, the text-prompt guided semi-supervised strategy integrates GroundedSAM [18] and LiDAR points with bbox annotation to generate pseudo-labels, enabling cost-effective training with mixed ground truth data.

Extensive experiments on OmniHD-Scenes [4] datasets demonstrate that MetaOcc achieves superior performance compared to existing methods, while our semi-supervised strategy maintains competitive accuracy with substantially reduced annotation.

Our contributions can be summarized as follows:

- We propose MetaOcc, the first work to efficiently fuse surround-view 4D radar and camera for occupancy prediction. Experiments show our method achieves state-of-the-art performance on OmniHD-Scenes datasets.
- We address sparse radar point cloud extraction with RHS, designing MFM that integrates LAF for adaptively capturing modality contribution and GCF for misalignment cross-modal feature fusion.
- We first develop a transferable semi-supervised learning strategy that leverages open-set segmentor for pseudo-label generation, significantly reducing annotation costs while maintaining competitive performance.

II. RELATED WORKS

A. Occupancy Prediction Approach

3D occupancy prediction advances scene understanding through dense geometric-semantic representation. Classical camera-based approaches [15], [19], [20] leverage 3D-based attention and depth-based modules for spatial features extraction, while BEV-based approaches [21], [22] trade spatial resolution for computational efficiency through height compression. TPVFormer [23] extends BEV to tri-perspective view with cross-view attention, while SparseOcc [24] introduces fully sparse 3D networks. Multi-modal approaches [13], [25], [26] predominantly focus on camera-LiDAR fusion through feature concatenation or attention mechanisms. Recent advances explore geometric-semantic awareness [12], diffusion denoising [27], and temporal enhancement [28] to improve fusion effect. The complementary characteristics of 4D imaging radar and cameras show promising potential for occupancy prediction [4], yet related research remains limited.

B. Occupancy Label Generation

Common methods [13], [15], [29] for generating 3D occupancy ground truth achieve high-quality semantic labels through point-wise LiDAR segmentation, yet require prohibitive annotation costs. Notably, OmniHD-Scenes dataset [4] extends pipeline that enhances semantic density of dynamic object features using non-keyframe point clouds without additional manual labeling. To address the labeling challenge, self-supervised approaches [16], [17] leverage neural rendering and geometric consistency. However, the unsupervised solutions face notable limitations in dynamic scenes and complex environments. Semi-supervised learning presents a promising direction by integrating open-set segmentor and LiDAR points with bbox annotation to generate pseudo-labels, enabling cost-effective training with mixed ground truth data.

III. METHOD

A. Overview

We propose MetaOcc, a surround-view occupancy prediction framework that fuses 4D radar and camera, as illustrated in Fig. 2. Multi-modal Spatial features are extracted independently through feature extractors. Subsequently, the extracted 3D features are processed by the MetaOcc Fusion Module (MFM), which employs local-global fusion mechanism to achieve efficient cross-modal integration. Finally, historical feature is incorporated through Temporal Alignment and Fusion (TAF) module before being fed into the occupancy head. To reduce annotation costs while maintaining performance, we further develop a semi-supervised training strategy that effectively combines ground truth and generated pseudo-labels.

B. Camera & 4D Radar Feature Extractor

The feature extraction stage incorporates a dual-stream architecture to process camera and 4D radar, independently.

Camera stream. The multi-view images are first processed through a 2D backbone network to extract features $F_I \in \mathbb{R}^{N_c \times C_I \times H_I \times W_I}$, where N_c denotes the number of cameras, and C_I , H_I , and W_I represent the channel dimension, height, and width of image features, respectively. Different from conventional projection methods [13], we adopt 2D to 3D spatial attention mechanism [15], [21] based on multi-scale deformable attention to achieve cross-view feature interaction. Through spatial attention, F_I are transformed into 3D features $F_c \in \mathbb{R}^{C \times H \times W \times Z}$, where W , H , and Z correspond to resolution of occupancy ground truth. Furthermore, F_c are further refined through camera encoder based on 3D convolutions, which progressively integrates multi-scale features to enhance spatial representation.

4D radar stream. Inherent sparsity of 4D radar results in insufficient occupancy density, which significantly impacts the performance of voxel-based methods [30] and limits effective 3D feature extraction. Although BEV-based solutions are simple and effective, direct application to 3D feature extraction remains challenging. While existing attempts to extend BEV features into 3D space via channel to height plugin (CHP) [22] or interpolation techniques [14] seem straightforward, they often degrade geometric feature fidelity.

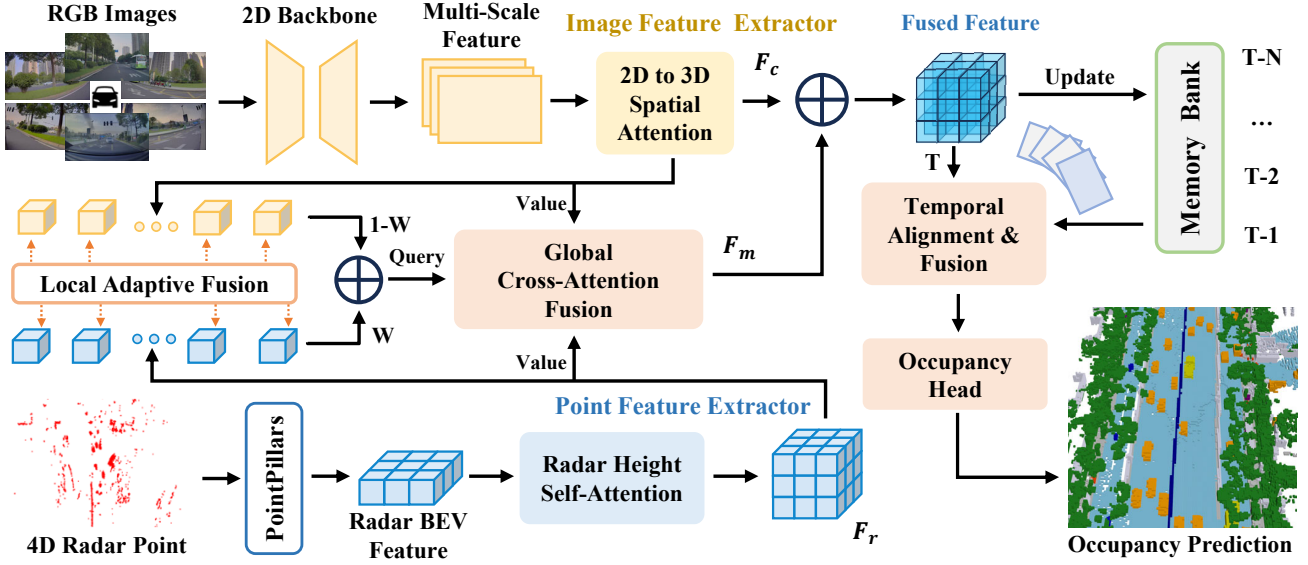


Fig. 2: Architecture of our MetaOcc framework. (a) Multi-view images are transformed into 3D features through the image feature extractor. (b) 4D radar point clouds processed by PointPillars are further enhanced through the designed Radar Height Self-Attention (RHS) module. (c) Multi-modal features are efficiently fused based on Local Adaptive Fusion (LAF) and Global Cross-Attention Fusion (GCF). (d) Temporal Alignment and Fusion (TAF) module aligns and fuses long-sequence features for occupancy prediction.

Inspired by [14], we propose a BEV-based solution called Radar Height Self-Attention (RHS) for 4D radar feature extraction, as illustrated in Fig. 3. We first employ PointPillars [31] to transform the input radar point clouds into BEV features $F_p^{bev} \in \mathbb{R}^{C \times H \times W}$. Then, F_p^{bev} is expanded along the Z-axis to initialize the radar 3D features $F_r^{ini} \in \mathbb{R}^{C \times H \times W \times Z}$. This expansion process can be formulated as:

$$F_r^{ini} = \text{Expand}(F_p^{bev}, Z) \quad (1)$$

where $\text{Expand}(\cdot, Z)$ denotes the operation that repeats the input features Z times along the Z-axis.

However, the simple expansion operation fails to capture feature distributions. Moreover, considering that elements with distinctive features in F_p^{bev} require varying attention weights along the vertical direction, we propose self-attention mechanism to address this problem. The learnable height positional encoding $P_h \in \mathbb{R}^{C \times Z}$ is first expanded to $P_h^e \in \mathbb{R}^{C \times H \times W \times Z}$ to match the dimensions of the shared features F_r^{ini} . Then, attention-based features F_r^{att} is obtained through an attention mechanism with positional encoding, as shown in:

$$F_r^{att} = \text{Conv}(F_r^{ini} \odot \sigma(\mathcal{G}_r(F_r^{ini} + P_h^e))) \quad (2)$$

where \odot denotes element-wise product, \mathcal{G}_r is a multi-layer 3D convolution, and σ represents the Sigmoid function for generating feature weights W_r . Finally, we employ residual connection to combine the F_r^{ini} and F_r^{att} , followed by further encoding:

$$F_r = \text{RadarEncoder}(F_r^{ini} + F_r^{att}) \quad (3)$$

where RadarEncoder consists of multiple blocks of 3D convolution layers with Softplus activation.

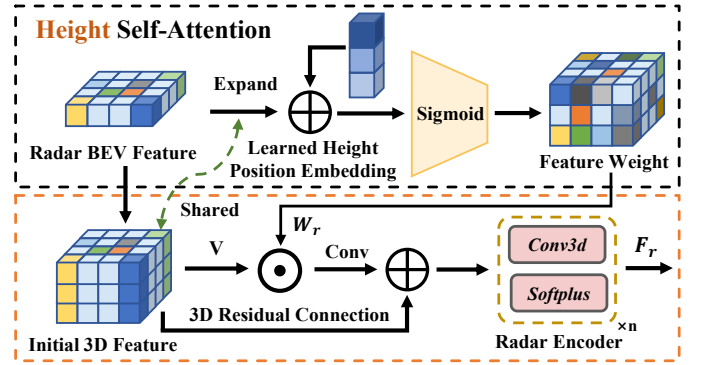


Fig. 3: The schema of Radar Height Self-Attention (RHS) for effective spatial feature extraction from sparse 4D radar point clouds.

C. MetaOcc Fusion Module

MetaOcc Fusion Module combines Local Adaptive Fusion (LAF) and Global Cross-Attention Fusion (GCF). LAF addresses the limitations of simple fusion strategies as concatenation in capturing modal contributions, while GCF handles spatio-temporal misalignment through deformable attention mechanism for learnable dynamic feature offsets. This cascaded design achieves comprehensive cross-modal feature fusion for occupancy prediction.

Local Adaptive Fusion. The LAF module employs an adaptive fusion mechanism to integrate 3D features F_c and F_r using a lightweight convolutional network. By concatenating multi-modal features and learning adaptive weights $W_{laf} \in \mathbb{R}^{C \times H \times W \times Z}$ through convolution layers [13], our design effectively combines semantic features from visual perception and robust geometric representations from radar

measurements. As a result, the proposed TAF enables to flexibly emphasize more reliable features from either modality while maintaining computational efficiency. The LAF strategy can be formulated as:

$$W_{laf} = \sigma(\mathcal{F}_w(\text{Concat}[F_c, F_r])) \quad (4)$$

$$F_{laf} = W_{laf} \odot F_c + (1 - W_{laf}) \odot F_r \quad (5)$$

where $\mathcal{F}_w(\cdot)$ represents a visibility weight encoder with 3D convolutions and normalization layers. The weight W_{laf} ranges from 0 to 1, automatically determining the contribution of each modality. The LAF achieves adaptive feature integration through efficient modality weighting, motivating us to further explore robust cross-modal fusion under spatio-temporal misalignment.

Global Cross-Attention Fusion. To address potential spatial-temporal misalignment caused by calibration errors and sensor latency, we introduce Global Cross-Attention Fusion (GCF) module that employs deformable attention with learnable offsets to dynamically fuse multi-modal features. Given that feature interaction in 3D space is computationally intensive, we project 3D features into BEV representation:

$$F^{bev} = \text{Linear}(\mathcal{H}(F^{3D})) \quad (6)$$

where Linear represents linear layer and $\mathcal{H}(\cdot)$ denotes height to channel operator, generating BEV features $F^{bev} \in \mathbb{R}^{C' \times H \times W}$ with flattened channel dimension $C' = C \times Z$.

Furthermore, GCF is designed as a powerful dual-stream architecture that not only processes modality-specific features independently but also facilitates comprehensive cross-modal interactions. Each stream incorporates distinct learnable BEV positional encodings $P_{k \in \{c,r\}} \in \mathbb{R}^{C' \times H \times W}$ for camera and radar inputs respectively, which effectively captures contextual information from both modalities. For initialization, we leverage F_{laf}^{bev} projected from F_{laf} as queries, which significantly enhances learning efficiency and feature extraction capability. Finally, the multi-modal features with dynamic offsets from dual streams are aggregated for further processing. The GCF can be mathematically expressed as:

$$F_m = \text{Conv}(\mathcal{H}'(\text{Norm}(\sum_{k \in \{c,r\}} \text{MDA}(F_{laf}^{bev}, F_k^{bev}), P_k)) + F_{laf}) \quad (7)$$

where MDA represents the multi-head deformable attention, F_k^{bev} denotes the BEV features from camera ($k = c$) and radar ($k = r$) modalities respectively, after view transformation. $\mathcal{H}'(\cdot)$ represents channel to height operator that reshapes BEV features into 3D representation.

D. Temporal Alignment and Fusion

Temporal fusion is crucial for occupancy prediction, especially in occluded environments. Inspired by [32], we design TAF module for effective temporal feature integration, as illustrated in Fig. 5. Given the 3D features of the sequence $\{F_t, F_{t-k}, \dots, F_{t-n}\} \in \mathbb{R}^{C \times H \times W \times Z}$, TAF first initializes F_{ini} at timestamp t . For historical alignment, F_{ini} are transformed to previous frames through coordinate transformation $\mathcal{T}(\cdot)$ with global pose $\mathcal{P}_{t \rightarrow (t-k)}$, where trilinear grid

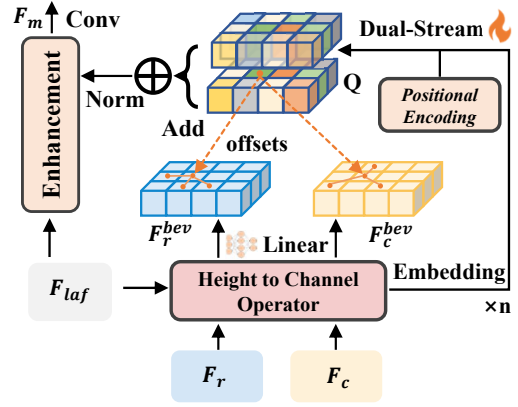


Fig. 4: Architecture of Global Cross-Attention Fusion (GCF). Multi-modal 3D features are projected to BEV through height to channel operator and enhanced by dual-stream deformable attention mechanism to handle spatio-temporal misalignment.

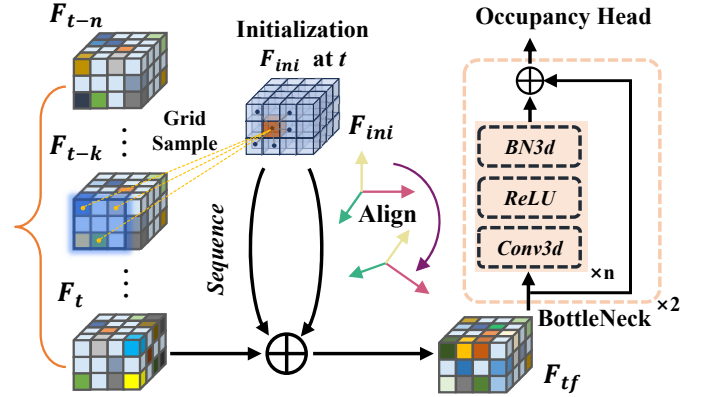


Fig. 5: Temporal Alignment and Fusion (TAF) module, which efficiently aligns and integrates 3D temporal features.

sample \mathcal{G}_t is employed to obtain features $F_{(t-k) \rightarrow t}$. Finally, we concatenate and refine the spatially-aligned features $\{F_t, F_{(t-k) \rightarrow t}, \dots, F_{(t-n) \rightarrow t}\}$ to produce temporal-enhanced feature F . The transformation and fusion process can be formulated as:

$$F_{(t-k) \rightarrow t} = \mathcal{G}_t(\mathcal{T}(F_{ini}, \mathcal{P}_{t \rightarrow (t-k)})) \quad (8)$$

$$F = \text{Bottleneck}(\text{Concat}[F_t, \dots, F_{(t-n) \rightarrow t}]) \quad (9)$$

where $\text{Bottleneck}(\cdot)$ consists of 3D convolution layers with ReLU activation and batch normalization.

E. Occupancy Head

The occupancy prediction head consists of linear layers that map fused multi-modal features to occupancy distributions. Subsequently, we integrate cross-entropy loss \mathcal{L}_{ce} for basic supervision, while lovasz-softmax loss [13] \mathcal{L}_{lovasz} and scene-class affinity losses [33] \mathcal{L}_{scal}^{geo} and \mathcal{L}_{scal}^{sem} are introduced to enhance both geometric and semantic consistency. The overall loss function is formulated as:

$$\mathcal{L} = \lambda_1 \mathcal{L}_{ce} + \lambda_2 \mathcal{L}_{lovasz} + \lambda_3 \mathcal{L}_{scal}^{geo} + \lambda_4 \mathcal{L}_{scal}^{sem} \quad (10)$$

where $\lambda_1, \lambda_2, \lambda_3, \lambda_4$ are loss weights of 1, 5, 1, 1.

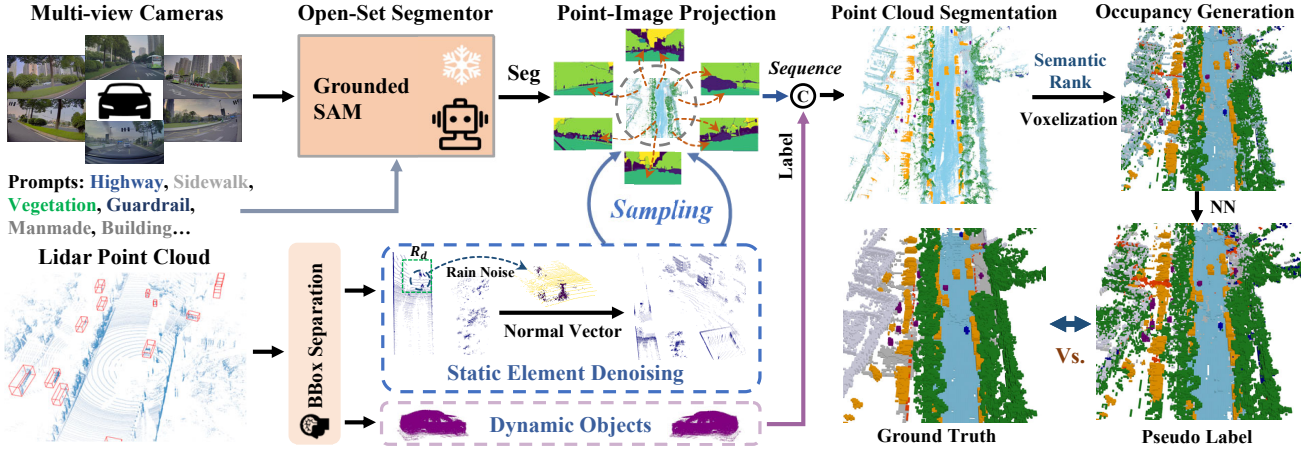


Fig. 6: Pseudo-label generation pipeline. (a) Zero-shot multi-view semantic segmentation is performed through Grounded-SAM with fine-tuned text prompts. (b) LiDAR point cloud is first divided into dynamic objects and static elements using bbox. Feature-based filtering is then applied in coarse drivable region R_d to eliminate rain noise. Finally, point cloud segmentation is achieved through point-image projection. (c) Temporal aggregation enhances semantic consistency and handles occlusions. (d) Occupancy label generation through knowledge-guided semantic voxelization and nearest neighbor algorithm.

F. Pseudo-Label Generation Approach for Semi-Supervised Training Procedure

Considering the advances of open-set segmentor in semantic understanding, we propose a semi-supervised framework for generating high-quality occupancy pseudo-labels. As shown in Fig. 6, our method takes multi-view images and LiDAR sequences as input to generate semantic occupancy representations through text-prompt guidance. The detailed pipeline is presented in Algorithm 1.

Image Semantic Segmentation. Pre-trained on over 10M images, Grounded-SAM [18] demonstrates strong zero-shot segmentation ability with flexible semantic control. We fine-tune the prompts \mathcal{T} specifically for static scene elements, and apply the model to segment multi-view images \mathcal{I} into detailed semantic masks I_k^{seg} .

LiDAR Semantic Segmentation. Similar to the OmniHD-Scenes [4] dataset, we use \mathcal{B} to separate dynamic objects D_{obj} and static element S_{ele} from LiDAR point clouds in keyframes. Furthermore, OmniHD-Scenes utilizes interpolated boxes \mathcal{B}^* to extract D_{obj} in non-keyframes, combined with iterative closest point to reduce spatial alignment errors. We extend the interpolated boxes to separate S_{ele} in non-keyframes, and further refine \mathcal{B}^* by computing maximum velocity errors between adjacent keyframes to minimize noise. Under normal conditions, separated S_{ele} are projected onto I_k^{seg} to obtain labels S^{seg} , where confidence-rank resolves multi-view semantic conflicts. However, conventional radius and voxel-based filtering fail to remove substantial noise around vehicles in rainy conditions, severely degrading label quality. We propose a feature-based filtering approach to address this challenge. First, we obtain a coarse drivable region R_d based on ego-vehicle position and nearby interpolated boxes \mathcal{B}^* . Then, we apply normal estimation of S_{ele} to identify ground semantics within R_d , effectively removing non-ground semantic noise and producing clean static elements S_{ele}^* , as shown in Fig. 6.

Temporal Enhancement. To address occlusion problems, we accumulate sequential information through temporal aggregation. Dynamic objects D_{seq} are assembled based on tracking IDs, while static elements are aligned and concatenated in the global coordinate system \mathcal{L}^{seg} using pose information \mathcal{P} .

Occupancy Generation. We transform \mathcal{L}^{seg} to local frame P^{seg} , then generate occupancy pseudo-labels $\hat{\mathcal{O}}$ through knowledge-guided semantic voxelization with occlusion complexity priors, followed by nearest neighbor matching.

Algorithm 1 Pseudo-Label Generation Pipeline

Input: Multi-view images Sequence \mathcal{I} , Lidar Sequence \mathcal{L} , Text prompts \mathcal{T} , Poses \mathcal{P} , Keyframe boxes \mathcal{B} .

Output: Occupancy pseudo-labels $\hat{\mathcal{O}}$ with semantics

```

// Image Semantic Segmentation
for each image  $I_k \in \mathcal{I}, k \in \{f, fl, fr, b, bl, br\}$  do
     $I_k^{seg} \leftarrow \text{GroundedSAM}(I_k, \mathcal{T})$ 
end for
// LiDAR Semantic Segmentation
Allframe boxes  $\mathcal{B}^* \leftarrow \text{Interpolate}(\mathcal{B}, \text{uniform velocity})$ 
for each point cloud  $P \in \mathcal{L}$  do
     $R_d \leftarrow D_{obj} \leftarrow \text{ExtractObject}(P, \mathcal{B}^*)$ 
     $S_{ele} \leftarrow \text{Separate}(P, D_{obj})$ 
     $S_{ele}^* \leftarrow \text{NormalEstimation}(S_{ele}, R_d) \triangleright \text{Rain Noise}$ 
     $S^{seg} \leftarrow \text{Point-Image Projection}(S_{ele}^*, I_k^{seg})$ 
end for
// Temporal Enhancement
 $D_{seq} \leftarrow \text{SequenceAgg}(D_{obj}, \text{ID})$ 
for each  $S_{ele}^*$  do
     $\mathcal{L}^{seg} \leftarrow \text{Concat}(\text{TransformToGlobal}(S^{seg}, \mathcal{P}))$ 
end for
// Occupancy Pseudo-Label Generation
 $P^{seg} \leftarrow \text{Concat}(\text{TransformToLocal}(\mathcal{L}^{seg}, \mathcal{P}), D_{seq})$ 
 $V_{seg} \leftarrow \text{Voxelization}(\text{SemanticRank}(P^{seg}))$ 
 $\hat{\mathcal{O}} \leftarrow \text{NearestNeighbor}(V_{seg}^{known}, V_{seg}^{unknown})$ 
return  $\hat{\mathcal{O}}$ 

```

TABLE I: Performance comparison of MetaOcc with state-of-the-art approaches on OmniHD-Scenes *test* set for 3D occupancy prediction. "C" and "R" denote camera and 4D radar modalities respectively. The last eleven columns represent IoU scores for different semantic categories. **Bold** and underlined values denote the best and second-best results, respectively.

Methods	Image Res.	Modality	Backbone	SC IoU	mIoU	car	pedestrian	rider	large vehicle	cycle	road obstacle	traffic fence	drive. surf.	sidewalk	vegetation	manmade
C-CONet [13] (ICCV 2023)	544×960	C	R50	25.69	13.42	20.03	3.51	11.71	16.62	0.79	1.14	22.75	33.57	14.82	17.73	4.93
SurroundOcc [15] (ICCV 2023)	544×960	C	R50	28.61	15.20	21.46	3.96	10.76	16.58	1.57	2.99	21.63	48.52	18.31	16.73	4.71
BEVFormer [21] (ECCV 2022)	544×960	C	R50	27.04	14.97	20.64	5.87	14.40	16.68	1.52	3.64	20.64	46.61	16.19	14.80	3.69
BEVFormer-T [21] (ECCV 2022)	544×960	C	R50	28.42	16.23	22.73	5.45	14.70	18.21	3.09	3.87	21.54	48.15	17.58	17.77	5.48
PanoOcc [32] (CVPR 2024)	544×960	C	R50	26.36	15.20	22.42	5.91	13.58	17.98	3.11	3.36	21.46	50.47	15.90	11.20	1.80
BEVFormer [21] (ECCV 2022)	864×1536	C	R101-DCN	28.30	16.41	23.72	6.37	16.33	20.44	1.78	3.78	22.21	48.55	17.88	15.49	3.99
BEVFormer-T [21] (ECCV 2022)	864×1536	C	R101-DCN	29.74	17.49	24.90	6.48	16.45	21.49	2.87	4.62	22.51	49.92	18.59	18.53	5.96
BEVFusion [25] (NeurIPS 2022)	544×960	C&R	R50	27.02	16.24	<u>27.02</u>	4.78	21.71	21.59	1.55	2.78	25.21	44.35	12.32	13.06	4.25
M-CONet [13] (ICCV 2023)	544×960	C&R	R50	27.74	16.08	25.21	3.42	17.53	21.46	0.88	0.58	29.88	34.48	14.89	19.57	8.98
MetaOcc-S (ours)	544×960	C&R	R50	31.52	20.92	26.87	7.21	23.44	23.55	3.96	5.92	37.22	49.07	19.41	20.98	12.46
MetaOcc (ours)	544×960	C&R	R50	32.75	21.73	27.52	8.84	24.06	<u>23.35</u>	4.79	6.47	38.75	<u>50.29</u>	19.91	21.88	13.22

IV. EXPERIMENTS

A. Implementation Details

Dataset. The OmniHD-Scenes dataset consists of 1.5K sequences captured by six multi-view cameras and 4D radars under diverse driving scenarios. Currently, the dataset include 200 annotated sequences totaling 11921 key-frames with comprehensive occupancy ground truth labels, enabling the evaluation of multi-modal occupancy prediction. Based on OmniHD-Scenes, we construct OmniHD-SemiOcc dataset through a semi-supervised learning strategy that combines varying proportions of ground truth with generated pseudo-labels to reduce annotation efforts.

Metrics. Both OmniHD-Scenes and OmniHD-SemiOcc benchmarks employ mean Intersection over Union (mIoU) for semantic accuracy and Scene Completion IoU (SC IoU) for geometric accuracy. The IoU metrics are formulated as:

$$\text{IoU} = \frac{TP}{TP + FP + FN} \quad (11)$$

$$\text{mIoU} = \frac{1}{C} \sum_{i=1}^C \frac{TP_i}{TP_i + FP_i + FN_i} \quad (12)$$

where TP , FP , and FN denote true positives, false positives, and false negatives respectively, and C represents the number of semantic classes. SC IoU is calculated between free and occupied space.

Network Settings. The prediction range is limited to $(-60, 60)$ m, $(-40, 40)$ m, and $(-3, 5)$ m along X -, Y -, and Z -axes, respectively. For the camera stream, we adopt ResNet50 [34] with FPN [35] as the 2D backbone, where input multi-view images are resized to 544×960 . The 4D radar features are encoded from three consecutive sweeps, containing spatial coordinates (x, y, z) , velocity components (v_x, v_y) , radar amplitude power, signal-to-noise ratio (SNR) and temporal information. The occupancy voxel size and spatial resolution are 0.5m and $160 \times 240 \times 16$, respectively.

Training Details. Our model is implemented based on MMDetection3D framework [36] and trained on NVIDIA GeForce RTX3090 GPUs with a batch size of 1. After initializing 2D backbone of the camera stream with FCOS3D [37] pre-trained weights, we adopt end-to-end training strategy for 12 epochs using AdamW optimizer with an initial learning rate of $2e-4$.

B. Main Results

To validate the effectiveness of our proposed MetaOcc and semi-supervised training procedure, extensive experiments are performed on OmniHD-Scenes datasets.

Full supervision results on OmniHD-Scenes Dataset. We compare MetaOcc with other methods on the OmniHD-Scenes dataset. All fusion-based methods adopt ResNet-50 backbone and 544×960 input resolution for fair comparison. As shown in Table I, our MetaOcc achieves superior performance with 32.75 SC IoU and 21.73 mIoU, surpassing previous methods by a large margin. Among camera-only methods, SurroundOcc achieves 28.61 SC IoU and 15.20 mIoU, while BEVFusion and M-CONet obtain 27.02 and 27.74 SC IoU with radar fusion respectively. MetaOcc outperforms SurroundOcc by improvements of 4.14 SC IoU and 6.53 mIoU, and surpasses M-CONet with gains of 5.01 SC IoU and 5.65 mIoU. MetaOcc demonstrates consistent improvements across semantic categories, particularly in challenging categories including rider and traffic fence, validating the effectiveness of our multi-modal feature fusion. Furthermore, our single-frame version MetaOcc-S achieves 31.52 SC IoU and 20.92 mIoU, surpassing BEVFormer which uses R101-DCN backbone at 864×1536 resolution, demonstrating the robustness of our approach.

Semi-supervision results on OmniHD-Scenes Dataset. To investigate the effectiveness of semi-supervised learning, we evaluate MetaOcc with varying proportions of ground truth (GT) and pseudo annotations on OmniHD-Scenes *test* set. As shown in Table II, MetaOcc achieves 32.38 SC IoU and 14.46

TABLE II: Evaluation results of MetaOcc on OmniHD-Scenes *test* set, where the model is trained on OmniHD-SemiOcc dataset. GT Ratio represents the proportion of ground truth in the training data.

GT Ratio	SC IoU	mIoU	car	pedestrian	rider	large vehicle	cycle	road obstacle	traffic fence	drive. surf.	sidewalk	vegetation	manmade
0%	32.38	14.46	25.59	7.92	20.92	23.22	0.96	0.77	5.28	41.10	6.49	18.71	8.09
25%	32.64	16.00	26.14	8.11	20.73	23.33	1.54	1.82	8.79	42.91	12.47	20.05	10.14
33%	32.76	16.49	25.98	8.41	21.12	22.12	1.80	1.66	10.17	44.64	14.66	19.85	10.96
50%	33.16	20.12	27.18	8.15	22.04	24.15	2.53	3.15	33.49	<u>49.87</u>	17.80	20.87	12.10
67%	<u>33.08</u>	21.04	27.53	8.12	22.69	23.37	3.78	4.98	<u>37.94</u>	49.76	19.16	21.28	12.80
75%	<u>32.97</u>	<u>21.22</u>	27.48	8.35	<u>23.06</u>	23.94	<u>3.76</u>	5.88	<u>37.25</u>	49.38	19.88	<u>21.35</u>	<u>13.14</u>
100%	32.75	21.73	<u>27.52</u>	8.84	24.06	23.35	4.79	6.47	38.75	50.29	19.91	21.88	13.22

mIoU with pseudo-labels alone, approaching the performance of fully supervised models using only cameras. As the GT ratio increases, mIoU demonstrates consistent yet diminishing improvements, peaking with a gain of 3.63 at 50%, reflecting the decreasing marginal benefit. Interestingly, the geometric metric SC IoU peaks at 50% with 33.16 and then decreases slightly, because non-keyframe pseudo-labels enhance density but introduce increasing noise. Notably, our model achieves 92.5% of the fully-supervised mIoU performance with only 50% GT annotations, demonstrating the effectiveness of our semi-supervised strategy.

C. Ablation Study

To evaluate the effectiveness of component in MetaOcc, we conduct ablation experiments on the OmniHD-Scenes dataset. The overall ablation results are summarized in Table III, where the baseline uses voxel-based 3D backbone [30] and addition fusion. Performance progressively improves with the inclusion of each module, as will be discussed in detail later.

Ablation of RHS. To evaluate effective 4D radar feature extraction, we compare our RHS module with voxel-based and BEV-based methods. As shown in Table IV, the voxel-based Second [30] achieves 32.52 SC IoU and 21.34 mIoU, while BEV-based PointPillars with expand operators obtain slightly lower SC IoU but higher mIoU of 32.17 and 21.64. This suggests voxel-based methods favor geometric features while BEV-based approaches excel in semantic extraction. Our RHS module achieves superior performance with 32.75 SC IoU and 21.73 mIoU by effectively combining the advantages of voxel-based and BEV-based paradigms through height self-attention mechanism.

Ablation of MFF. The ablation studies of LAF and GCF demonstrate the effectiveness of our MFF design. Building upon RHS, LAF module further improves performance to 32.48 SC IoU and 21.36 mIoU through adaptive feature integration. The significant gains (+0.55 SC IoU, +0.41 mIoU) demonstrate the capability of LAF in capturing fine-grained local correspondences between modalities. GCF module further improves performance to 32.75 SC IoU and 21.73 mIoU through dual-stream deformable attention. The consistent improvements (+0.27 SC IoU, +0.37 mIoU) demonstrate the

TABLE III: ablation study of MetaOcc.

RHS	LAF	GCF	SC IoU	mIoU
			31.12	19.60
✓			31.93	20.95
✓	✓		<u>32.48</u>	<u>21.36</u>
✓	✓	✓	32.75	21.73

TABLE IV: Ablation study of RHS.

Method	SC IoU	mIoU
Second [30]	<u>32.52</u>	21.34
PointPillars + Expand	32.17	<u>21.64</u>
PointPillars + RHS (ours)	32.75	21.73

capability of GCF in handling spatio-temporal misalignment through global cross-modal interaction.

Ablation of TAF. We conduct an ablation study on the temporal length T of TAF module in Table V. The TAF module effectively aggregates temporal features, where increasing temporal length from 1 to 2 brings significant improvements (+1.23 SC IoU, +0.81 mIoU), while the gain from 2 to 3 frames is relatively marginal (+0.45 SC IoU, +0.33 mIoU). Since longer sequences require more training time and memory usage, we set $T = 3$ as the default configuration balancing accuracy and computational cost.

V. CONCLUSIONS

In this work, we propose MetaOcc, a novel multi-modal occupancy prediction framework that effectively fuses surround-view cameras and 4D radar with excellent attention mechanisms. We first develop RHS to extract 3D features from sparse 4D radar points. Then, LAF and GCF are employed to capture modality contribution and address potential spatio-temporal misalignment. Afterward, we introduce TAF to integrate historical features. Extensive experiments demonstrate that MetaOcc achieves superior performance in semantic and geometric accuracy on the OmniHD-Scenes dataset. Additionally, our semi-supervised training strategy with open-set segmentor model significantly reduces annotation dependency while maintaining robust performance.

TABLE V: Ablation study of TAF.

Length	SC IoU	mIoU
T = 1	31.52	20.92
T = 2	32.48	21.38
T = 3	32.75	21.73

REFERENCES

- [1] F. Ding, X. Wen, Y. Zhu, Y. Li, and C. X. Lu, "RadarOcc: Robust 3d occupancy prediction with 4d imaging radar," *Advances in Neural Information Processing Systems (NeurIPS)*, 2024.
- [2] H. Xu, J. Chen, S. Meng, Y. Wang, and L.-P. Chau, "A survey on occupancy perception for autonomous driving: The information fusion perspective," *Information Fusion*, vol. 114, p. 102671, 2025.
- [3] J. Liu, Q. Zhao, W. Xiong, T. Huang, Q.-L. Han, and B. Zhu, "SMURF: Spatial multi-representation fusion for 3d object detection with 4d imaging radar," *IEEE Transactions on Intelligent Vehicles*, vol. 9, no. 1, pp. 799–812, 2024.
- [4] L. Zheng, L. Yang, Q. Lin, W. Ai, M. Liu, S. Lu, J. Liu, H. Ren, J. Mo, X. Bai, *et al.*, "OmniHD-Scenes: A next-generation multimodal dataset for autonomous driving," *arXiv preprint arXiv:2412.10734*, 2024.
- [5] R. Guan, L. Jia, F. Yang, S. Yao, E. Purwanto, X. Zhu, E. G. Lim, J. Smith, K. L. Man, X. Hu, *et al.*, "WaterVG: Waterway visual grounding based on text-guided vision and mmwave radar," *IEEE Transactions on Intelligent Transportation Systems*, pp. 1–17, 2025.
- [6] L. Zheng, S. Li, B. Tan, L. Yang, S. Chen, L. Huang, J. Bai, X. Zhu, and Z. Ma, "RCFusion: Fusing 4-d radar and camera with bird's-eye view features for 3-d object detection," *IEEE Transactions on Instrumentation and Measurement*, vol. 72, pp. 1–14, 2023.
- [7] R. Guan, J. Liu, L. Jia, H. Zhao, S. Yao, X. Zhu, K. L. Man, E. G. Lim, J. Smith, and Y. Yue, "NanoMVG: Usv-centric low-power multi-task visual grounding based on prompt-guided camera and 4d mmwave radar," *arXiv preprint arXiv:2408.17207*, 2024.
- [8] W. Xiong, J. Liu, T. Huang, Q.-L. Han, Y. Xia, and B. Zhu, "LXL: Lidar excluded lean 3d object detection with 4d imaging radar and camera fusion," *IEEE Transactions on Intelligent Vehicles*, vol. 9, no. 1, pp. 79–92, 2024.
- [9] R. Guan, R. Zhang, N. Ouyang, J. Liu, K. L. Man, X. Cai, M. Xu, J. Smith, E. G. Lim, Y. Yue, *et al.*, "Talk2Radar: Bridging natural language with 4d mmwave radar for 3d referring expression comprehension," *arXiv preprint arXiv:2405.12821*, 2024.
- [10] L. Zheng, Z. Ma, X. Zhu, B. Tan, S. Li, K. Long, W. Sun, S. Chen, L. Zhang, M. Wan, *et al.*, "TJ4DRadSet: A 4d radar dataset for autonomous driving," in *IEEE 25th International Conference on Intelligent Transportation Systems (ITSC)*, 2022, pp. 493–498.
- [11] A. Palffy, E. Pool, S. Baratam, J. F. Kooij, and D. M. Gavrilu, "Multi-class road user detection with 3+1d radar in the view-of-delift dataset," *IEEE Robotics and Automation Letters*, vol. 7, no. 2, pp. 4961–4968, 2022.
- [12] J. Pan, Z. Wang, and L. Wang, "Co-occ: Coupling explicit feature fusion with volume rendering regularization for multi-modal 3d semantic occupancy prediction," *IEEE Robotics and Automation Letters*, 2024.
- [13] X. Wang, Z. Zhu, W. Xu, Y. Zhang, Y. Wei, X. Chi, Y. Ye, D. Du, J. Lu, and X. Wang, "OpenOccupancy: A large scale benchmark for surrounding semantic occupancy perception," in *Proceedings of the IEEE/CVF International Conference on Computer Vision (ICCV)*, 2023, pp. 17 850–17 859.
- [14] Y. Zhang, Z. Zhu, and D. Du, "Occformer: Dual-path transformer for vision-based 3d semantic occupancy prediction," in *Proceedings of the IEEE/CVF International Conference on Computer Vision*, 2023, pp. 9433–9443.
- [15] Y. Wei, L. Zhao, W. Zheng, Z. Zhu, J. Zhou, and J. Lu, "SurroundOcc: Multi-camera 3d occupancy prediction for autonomous driving," in *Proceedings of the IEEE/CVF International Conference on Computer Vision (ICCV)*, 2023, pp. 21 729–21 740.
- [16] C. Zhang, J. Yan, Y. Wei, J. Li, L. Liu, Y. Tang, Y. Duan, and J. Lu, "Occnerf: Self-supervised multi-camera occupancy prediction with neural radiance fields," *arXiv preprint arXiv:2312.09243*, 2023.
- [17] Y. Liu, L. Mou, X. Yu, C. Han, S. Mao, R. Xiong, and Y. Wang, "Let occ flow: Self-supervised 3d occupancy flow prediction," *arXiv preprint arXiv:2407.07587*, 2024.
- [18] T. Ren, S. Liu, A. Zeng, J. Lin, K. Li, H. Cao, J. Chen, X. Huang, Y. Chen, F. Yan, *et al.*, "Grounded sam: Assembling open-world models for diverse visual tasks," *arXiv preprint arXiv:2401.14159*, 2024.
- [19] Y. Li, Z. Yu, C. Choy, C. Xiao, J. M. Alvarez, S. Fidler, C. Feng, and A. Anandkumar, "Voxformer: Sparse voxel transformer for camera-based 3d semantic scene completion," in *Proceedings of the IEEE/CVF conference on computer vision and pattern recognition*, 2023, pp. 9087–9098.
- [20] Z. Li, Z. Yu, W. Wang, A. Anandkumar, T. Lu, and J. M. Alvarez, "Fb-bev: Bev representation from forward-backward view transformations," in *Proceedings of the IEEE/CVF International Conference on Computer Vision*, 2023, pp. 6919–6928.
- [21] Z. Li, W. Wang, H. Li, E. Xie, C. Sima, T. Lu, Y. Qiao, and J. Dai, "BEV-Former: Learning bird's-eye-view representation from multi-camera images via spatiotemporal transformers," in *European Conference on Computer Vision (ECCV)*, 2022, pp. 1–18.
- [22] Z. Yu, C. Shu, J. Deng, K. Lu, Z. Liu, J. Yu, D. Yang, H. Li, and Y. Chen, "FlashOcc: Fast and memory-efficient occupancy prediction via channel-to-height plugin," *arXiv preprint arXiv:2311.12058*, 2023.
- [23] Y. Huang, W. Zheng, Y. Zhang, J. Zhou, and J. Lu, "Tri-perspective view for vision-based 3d semantic occupancy prediction," in *IEEE/CVF Conference on Computer Vision and Pattern Recognition (CVPR)*, 2023, pp. 9223–9232.
- [24] H. Liu, H. Wang, Y. Chen, Z. Yang, J. Zeng, L. Chen, and L. Wang, "Fully sparse 3d panoptic occupancy prediction," *arXiv preprint arXiv:2312.17118*, 2023.
- [25] T. Liang, H. Xie, K. Yu, Z. Xia, Z. Lin, Y. Wang, T. Tang, B. Wang, and Z. Tang, "BEVFusion: A simple and robust lidar-camera fusion framework," *Advances in Neural Information Processing Systems (NeurIPS)*, vol. 35, pp. 10 421–10 434, 2022.
- [26] Y. Shi, K. Jiang, K. Wang, K. Qian, Y. Wang, J. Li, T. Wen, M. Yang, Y. Xu, and D. Yang, "Effocc: A minimal baseline for efficient fusion-based 3d occupancy network," *arXiv preprint arXiv:2406.07042*, 2024.
- [27] G. Wang, Z. Wang, P. Tang, J. Zheng, X. Ren, B. Feng, and C. Ma, "Oc-cgen: Generative multi-modal 3d occupancy prediction for autonomous driving," in *European Conference on Computer Vision*. Springer, 2025, pp. 95–112.
- [28] Z. Lin, H. Jin, Y. Wang, Y. Wei, and N. Dong, "TEOcc: Radar-camera multi-modal occupancy prediction via temporal enhancement," in *27th European Conference on Artificial Intelligence (ECAI)*, 2024, pp. 129–136.
- [29] X. Tian, T. Jiang, L. Yun, Y. Mao, H. Yang, Y. Wang, Y. Wang, and H. Zhao, "Occ3d: A large-scale 3d occupancy prediction benchmark for autonomous driving," *Advances in Neural Information Processing Systems*, vol. 36, 2024.
- [30] Y. Yan, Y. Mao, and B. Li, "Second: Sparsely embedded convolutional detection," *Sensors*, vol. 18, no. 10, p. 3337, 2018.
- [31] A. H. Lang, S. Vora, H. Caesar, L. Zhou, J. Yang, and O. Beijbom, "PointPillars: Fast encoders for object detection from point clouds," in *Proceedings of the IEEE/CVF Conference on Computer Vision and Pattern Recognition (CVPR)*, 2019, pp. 12 697–12 705.
- [32] Y. Wang, Y. Chen, X. Liao, L. Fan, and Z. Zhang, "PanoOcc: Unified occupancy representation for camera-based 3d panoptic segmentation," in *Proceedings of the IEEE/CVF Conference on Computer Vision and Pattern Recognition (CVPR)*, 2024, pp. 17 158–17 168.
- [33] A.-Q. Cao and R. De Charette, "MonoScene: Monocular 3d semantic scene completion," in *Proceedings of the IEEE/CVF Conference on Computer Vision and Pattern Recognition (CVPR)*, 2022, pp. 3991–4001.
- [34] K. He, X. Zhang, S. Ren, and J. Sun, "Deep residual learning for image recognition," in *Proceedings of the IEEE Conference on Computer Vision and Pattern Recognition (CVPR)*, 2016, pp. 770–778.
- [35] T.-Y. Lin, P. Dollár, R. Girshick, K. He, B. Hariharan, and S. Belongie, "Feature pyramid networks for object detection," in *Proceedings of the IEEE Conference on Computer Vision and Pattern Recognition (CVPR)*, 2017, pp. 2117–2125.
- [36] M. Contributors, "Mmdetection3d: Openmmlab next-generation platform for general 3d object detection," 2020.
- [37] T. Wang, X. Zhu, J. Pang, and D. Lin, "FCOS3d: Fully convolutional one-stage monocular 3d object detection," in *Proceedings of the IEEE/CVF International Conference on Computer Vision (ICCV)*, 2021, pp. 913–922.